

Published in final edited form as:

*Chem Phys Lett.* 2014 July 21; 608: 303–307. doi:10.1016/j.cplett.2014.06.002.

## Nonlinear optical properties of multipyrrole dyes

**Mathieu Frenette<sup>2,\*</sup>, Maryam Hatamimoslehabadi<sup>1,\*</sup>, Stephanie Bellinger-Buckley<sup>2</sup>, Samir Laoui<sup>1</sup>, Seema Bag<sup>2</sup>, Olivier Dantiste<sup>1</sup>, Jonathan Rochford<sup>2</sup>, and Chandra Yelleswarapu<sup>1</sup>**

Jonathan Rochford: Jontham.rochford@umb.edu; Chandra Yelleswarapu: Chandra.yelleswarapu@umb.edu

<sup>1</sup>Department of Physics, University of Massachusetts Boston, Boston, MA 02125

<sup>2</sup>Department of Chemistry, University of Massachusetts Boston, Boston, MA 02125

### Abstract

The nonlinear optical properties of a series of pyrrolic compounds consisting of BODIPY and aza-BODIPY systems are investigated using 532 nm nanosecond laser and the Z-scan technique. Results show that 3,5-distyryl extension of BODIPY to the red shifted MeO<sub>2</sub>BODIPY dye has a dramatic impact on its nonlinear absorption properties changing it from a saturable absorber to an efficient reverse saturable absorbing material with a nonlinear absorption coefficient of  $4.64 \times 10^{-10}$  m/W. When plotted on a concentration scale per mole of dye in solution MeO<sub>2</sub>BODIPY far outperforms the recognized zinc(II) phthalocyanine dye and is comparable to that of zinc(II) tetraphenylporphyrin.

### Introduction

Materials with optimized nonlinear optical (NLO) properties have been the focus of fundamental and applied research in recent years.<sup>1</sup> A wide variety of materials including inorganic and organic semiconductors, natural and synthetic nanomaterials, molecular dyes, and polymer systems,<sup>2–9</sup> display nonlinear optical properties which have found use in variety of applications.<sup>10–16</sup> Organic nonlinear optical materials, in particular, have attracted major attention due to their wide scope and ability to maximize a nonlinear response by tailored modification of their molecular structure.<sup>17–25</sup> Established nonlinear optical organic materials such as the pyrrole-based porphyrins, phthalocyanines and aza/azo-benzenes, possess a large number of delocalized  $\pi$ -electrons, with band-gaps of 2–3 eV and reasonably high nonlinearities.<sup>26,27</sup> The 4,4-difluoro-4-bora-3a,4a-diaza-s-indacene chromophore, more commonly known as BODIPY and often regarded as “porphyrin’s little sister” due to its similarity to the tetrapyrrole macrocycle, is another established class of methine bridged dipyrrole chromophore with unique and attractive photophysical properties.<sup>28</sup> In general, organic NLO materials, and BODIPY in particular, offer the luxury of tunable, sharp, high oscillator strength absorption bands with potentially large two-photon excitation cross

© 2014 Elsevier B.V. All rights reserved.

\*Equal contribution

**Publisher's Disclaimer:** This is a PDF file of an unedited manuscript that has been accepted for publication. As a service to our customers we are providing this early version of the manuscript. The manuscript will undergo copyediting, typesetting, and review of the resulting proof before it is published in its final citable form. Please note that during the production process errors may be discovered which could affect the content, and all legal disclaimers that apply to the journal pertain.

sections ( $\sigma_2$ ).<sup>29–33</sup> For imaging applications in particular, focused near infrared femtosecond pulsed laser excitation is used to induce concerted two-photon  $S_0 \rightarrow S_1$  electronic excitation where efficient  $\sigma_2$  dyes have enabled a high optical contrast with an accurate three-dimensional spatial confinement.<sup>34–36</sup> In the nanosecond excitation regime, recent applications focus primarily on the optical limiting properties of dye molecules achieved by singlet ( $S_1 \rightarrow S_2$ ) or triplet ( $T_1 \rightarrow T_2$ ) based excited state absorption following pulsed excitation of the ground to first excited state ( $S_0 \rightarrow S_1$ ) transition.

The pioneering work of Ziessel, Burgess and Akkaya, among others, has demonstrated how extension of  $\pi$ -conjugated substituents at the BODIPY 3,5-positions can give rise to substantial ( $> 100$  nm) red-shifts in the  $S_0 \rightarrow S_1$  electronic transition beyond 600 nm while maintaining a strong absorption coefficient ( $\epsilon \sim 10^5 \text{ M}^{-1} \text{ cm}^{-1}$ ).<sup>37</sup> Following similar structural modification to enhance the nonlinear absorption, here we report a series of  $\pi$ -conjugated pyrrole dyes with favorable tuning of excited state absorption properties. In fact, it is shown below that BODIPY which is a saturable absorber (SA) can be effectively converted to a reverse saturable absorbing (RSA) material upon such modification. Two photon and multiphoton absorption behavior is observed for the series of compounds 1,3,5,7-tetramethyl-6-(4-methylbenzoate)BODIPY (BODIPY); 1,7-dimethyl-3,5-bis(methoxy-4-styrylbenzene)-6-(4-methylbenzoate)BODIPY (MeO<sub>2</sub>BODIPY); 1,3,5,7-tetraphenyl-6-aza-BODIPY (aza-BODIPY); 1,7-diphenyl-3,5-bis(4-methoxyphenyl)-6-aza-BODIPY (MeO<sub>2</sub>-aza-BODIPY) using the conventional optical Z-scan technique.<sup>38</sup> Structures of bis- and tetra-pyrrole dyes, and their aza analogues, investigated in this study are shown in Fig. 1.

## Materials and Methods

Electronic absorption spectra were recorded in spectrophotometric grade tetrahydrofuran (Sigma) on an Agilent 8452 spectrometer in a standard 10.0 mm path length quartz cell. For Z-scan measurements a 2.0 mm path length quartz cell was placed at 45° with respect to the incident laser beam (effective path length = 2.83 mm). Samples with a linear absorption coefficient ( $\alpha_0$ ) of 345  $\text{m}^{-1}$  at the laser excitation wavelength 532 nm were prepared (optical density = 0.3). The output of a frequency doubled Nd:YAG laser (Continuum Minilite II, 532 nm, pulse width  $\sim 3$  ns) was focused on to the sample using a 18 cm focal length lens. The sample was mounted on an automated translation stage (Thorlabs NRT 150) and moved horizontally along the z direction through the focal point of the beam. The beam waist ( $\omega_0$ ) at focal plane was estimated to be  $57 \pm 5 \mu\text{m}$ . The energy incident on the sample was controlled by the combination of a half-wave plate and a linear polarizer. The incident laser energy before the focusing lens was  $\sim 65 \mu\text{J}$ . At the focal point, the sample experienced optimum pump intensity, which decreased gradually on either side of the focus. As the intensity of incident light changed, the optical transmittance varied according to the sample's nonlinear electronic absorption properties. Importantly, a linear of the optical detector was verified; laser transmittance was measured as a function of crystal violet concentration in tetrahydrofuran with varying transmittance from 0 to 1 at 532 nm; a correlation better than  $R^2 = 0.99$  was obtained when a neutral density filter of OD 1 was placed in front of the detector (data not shown).

## Results and discussion

An overlay of the UV/Vis/NIR absorption spectra for ZnTPP, ZnPc, BODIPY, MeO<sub>2</sub>BODIPY, aza-BODIPY and MeO<sub>2</sub>-aza-BODIPY is presented in Fig. 2. All dyes display a low energy S<sub>0</sub>→S<sub>1</sub> electronic absorption in the range 515 nm (BODIPY) to 693 nm (MeO<sub>2</sub>-aza-BODIPY) with comparable oscillator strengths ranging from 5 – 12 × 10<sup>4</sup> M<sup>-1</sup> cm<sup>-1</sup>. The electron rich aza derivatives, ZnPc and aza-BODIPYs, each show a significant red shift relative to their methine bridged counterparts, ZnTPP and BODIPY, respectively.

Open aperture Z-scan curves for all samples ( $\alpha_0 = 345 \text{ m}^{-1}$ , optical density = 0.3 @ 532 nm) are shown in Fig. 3, where lines represent theoretical fits to the experimental data. The experimental normalized transmission data fit well with nonlinear transmission equations.<sup>39</sup> The unmodified BODIPY system displays a typical SA character. Hence this data fits well to a SA transmittance equation, where the saturation intensity is  $1.25 \times 10^{11} \text{ W/m}^2$ . In contrast each of the functionalized and core modified BODIPYs show RSA behavior and are best fit to a RSA transmittance equation. To find the origin of this RSA behavior, the nonlinear absorption coefficient behavior was studied at various on-axis intensities ( $I_0$ ). Obtained Z-scan curves and the corresponding theoretical fits to the experimental data are shown in figure 4. The obtained  $\beta$  values are plotted with respect to  $I_0$  in figure 5. This clearly demonstrates how  $\beta$  decreases as  $I_0$  is increased, indicating that the observed RSA effect is due to excited state absorption involving the S<sub>1</sub> and S<sub>2</sub> electronic excited states.<sup>40</sup> A summary of nonlinear absorption coefficients are summarized in Table 1. It is also conclusive from the absorption coefficients that nonlinear absorption of the MeO<sub>2</sub>BODIPY system is superior to that of ZnPc and on par with ZnTPP.

Due to the difference in molar extinction coefficients ( $\epsilon$ ) of the compounds under study (Fig. 2), various concentrations had been used to achieve 0.3 absorbance at the laser operating wavelength of 532 nm (Table 1). To make a more meaningful comparison between the various dyes and estimate their contribution to the nonlinear absorption per molar concentration, i.e. to make a true qualitative comparison of nonlinear absorption efficiency at a structural level, the 'relative nonlinear absorption per mole' was calculated for each dye with respect to the Z position (Fig. 6). This transformation was achieved by subtracting the linear absorption (0.3 for each dye), dividing by dye concentration (mol L<sup>-1</sup>) and finally dividing by the maximum absorption response (ZnTPP at Z = 0) to allow a relative comparison of each structure for quantitative purposes. Figure 4 effectively shows which dyes are most efficient at absorbing an additional photon in their excited states with respect to the photon density (Z-position). Noteworthy, MeO<sub>2</sub>BODIPY is just as effective as the excellent ZnTPP nonlinear RSA dye. Furthermore, while the aza-BODIPY dyes are about half as efficient as MeO<sub>2</sub>BODIPY their nonlinear absorption behavior per mole is at least twice that of their established ZnPc macrocyclic counterpart. Such a plot allows a valuable side-by-side comparison to be made for a series of dyes which can inform on strategic design of future nonlinear absorbing materials for both biological imaging and optical limiting applications.

The power limiting behavior of MeO<sub>2</sub>BODIPY is shown in figure 7. Using the Z-scan setup discussed above, the sample was placed at  $z = 0$  (focal plane of the 18 cm focal length lens) and the transmitted energy was recorded as the incident energy was varied. The limiting threshold energy was  $\sim 200 \mu\text{J}$  and the output was clamped at  $\sim 25 \mu\text{J}$ .

## Conclusion

The nonlinear optical properties of styryl-BODIPY and aza-BODIPY dye systems show great promise towards the design of future NLO organic materials via an excited state (two-photon) absorption mechanism. In contrast, the unmodified BODIPY dye shows just saturable absorption character at the 532 nm wavelength used. Through designed structural modification in MeO<sub>2</sub>BODIPY not only has the BODIPY unit been converted into a reverse saturable absorption material, but its nonlinear absorption coefficient is now competitive with the established ZnTPP and ZnPc dyes.

## Acknowledgments

The authors thank UMass Boston and Dana-Farber/Harvard Cancer Center pilot project grant number U54CA156734 for financial support. CSY would like to thank Dr. I. M. Kislyakov, Saint-Petersburg National Research University of Information Technologies, Mechanics and Optics, Saint-Petersburg, Russia for valuable discussion.

## References

1. Christodoulides DN, Khoo IC, Salamo GJ, Stegeman GI, Van Stryland EW. Nonlinear refraction and absorption: mechanisms and magnitudes. *Advances in Optics and Photonics*. 2010; 2:60–200.
2. Anthony JK, et al. Particle size-dependent giant nonlinear absorption in nanostructured Ni-Ti alloys. *Optics express*. 2008; 16:11193–11202. [PubMed: 18648435]
3. Chan Y-P, Lin J-H, Hsu C-C, Hsieh W-F. Near-resonant high order nonlinear absorption of ZnO thin films. *Optics express*. 2008; 16:19900–19908. [PubMed: 19030077]
4. Ivanov IP, Li X, Dolan PR, Gu M. Nonlinear absorption properties of the charge states of nitrogen-vacancy centers in nanodiamonds. *Optics letters*. 2013; 38:1358–1360. [PubMed: 23595484]
5. Kiran PP, et al. Enhanced optical limiting and nonlinear absorption properties of azoarene-appended phosphorus (V) tetratolylporphyrins. *Applied optics*. 2002; 41:7631–7636. [PubMed: 12510931]
6. Wang K, et al. Nonlinear optical propagation in a tandem structure comprising nonlinear absorption and scattering materials. *Applied Physics Letters*. 2014; 104
7. Yelleswarapu CS, Gu G, Abdullayev E, Lvov Y, Rao D. Nonlinear optics of nontoxic nanomaterials. *Optics communications*. 2010; 283:438–441.
8. Yamashita S. A tutorial on nonlinear photonic applications of carbon nanotube and graphene. *Journal of Lightwave Technology*. 2012; 30:427–447.
9. Khoo IC. Nonlinear optics, active plasmonics and metamaterials with liquid crystals. *Progress in Quantum Electronics*. 2014
10. Haripadmam PC, John H, Philip R, Gopinath P. Enhanced optical limiting in polystyrene–ZnO nanotop composite films. *Optics letters*. 2014; 39:474–477. [PubMed: 24487843]
11. Four M, et al. A novel ruthenium(II) complex for two-photon absorption-based optical power limiting in the near-IR range. *Physical chemistry chemical physics : PCCP*. 2011; 13:17304–17312. [PubMed: 21879060]
12. Yelleswarapu C, et al. All-optical spatial filtering with power limiting materials. *Optics express*. 2006; 14:1451–1457. [PubMed: 19503469]
13. Zhou GJ, Wong WY. Organometallic acetylides of Pt(II), Au(I) and Hg(II) as new generation optical power limiting materials. *Chem Soc Rev*. 2011; 40:2541–2566. [PubMed: 21264386]

14. Christenson CW, Saini A, Valle B, Shan J, Singer KD. Nonlinear fluorescence modulation of an organic dye for optical data storage. *J. Opt. Soc. Am. B.* 2014; 31:637–641.
15. Andrade CD, Yanez CO, Rodriguez L, Belfield KD. A series of fluorene-based two-photon absorbing molecules: synthesis, linear and nonlinear characterization, and bioimaging. *The Journal of organic chemistry.* 2010; 75:3975–3982. [PubMed: 20481596]
16. De Boni L, Corrêa DS, Mendonça CR. *Nonlinear Optical Absorption of Organic Molecules for Applications in Optical Devices.* 2010
17. Mi Y, Liang P, Jin Z, Wang D, Yang Z. Synthesis and third-order nonlinear optical properties of triphenylene derivatives modified by click chemistry. *Chemphyschem : a European journal of chemical physics and physical chemistry.* 2013; 14:4102–4108. [PubMed: 24323854]
18. Ahn HY, Yao S, Wang X, Belfield KD. Near-Infrared-Emitting Squaraine Dyes with High 2PA Cross-Sections for Multiphoton Fluorescence Imaging. *ACS Appl Mater Interfaces.* 2012; 4:2847–2854. [PubMed: 22591003]
19. Dalton GT, et al. Organometallic complexes for nonlinear optics. 42. Syntheses, linear, and nonlinear optical properties of ligated metal-functionalized oligo(p-phenyleneethynylene)s. *Inorganic chemistry.* 2009; 48:6534–6547. [PubMed: 19548639]
20. Chen Z, et al. Photoresponsive J-aggregation behavior of a novel azobenzene-phthalocyanine dyad and its third-order optical nonlinearity. *The journal of physical chemistry. B.* 2008; 112:7387–7394. [PubMed: 18512976]
21. Belfield KD, Bondar MV, Hernandez FE, Przhonska OV, Yao S. Two-photon absorption cross section determination for fluorene derivatives: analysis of the methodology and elucidation of the origin of the absorption processes. *The journal of physical chemistry. B.* 2007; 111:12723–12729. [PubMed: 17939706]
22. Rath H, et al. Core-modified expanded porphyrins with large third-order nonlinear optical response. *Journal of the American Chemical Society.* 2005; 127:11608–11609. [PubMed: 16104730]
23. Bredas J, Adant C, Tackx P, Persoons A, Pierce B. Third-order nonlinear optical response in organic materials: theoretical and experimental aspects. *Chemical reviews.* 1994; 94:243–278.
24. Chemla, DS. *Nonlinear optical properties of organic molecules and crystals.* Elsevier; 2012.
25. Venugopal Rao S, et al. Two-photon and three-photon absorption in dinaphthoporphycenes. *Chemical Physics Letters.* 2011; 514:98–103.
26. Wei T, et al. Direct measurements of nonlinear absorption and refraction in solutions of phthalocyanines. *Applied Physics B.* 1992; 54:46–51.
27. Hosoda, M.; Wada, T.; Yamada, A.; Garito, AF.; Sasabe, H. *MRS Proceedings.* Vol. 175. Cambridge Univ Press; 1989. Enhancement of third order nonlinearity on phthalocyanine compounds.
28. Ulrich G, Ziessel R, Harriman A. *The Chemistry of Fluorescent Bodipy Dyes: Versatility Unsurpassed.* *Angewandte Chemie International Edition.* 2008; 47:1184–1201.
29. Liu X, et al. New insights into two-photon absorption properties of functionalized aza-BODIPY dyes at telecommunication wavelengths: a theoretical study. *Physical chemistry chemical physics : PCCP.* 2013; 15:4666–4676. [PubMed: 23435838]
30. Wang JN, et al. An accurate and efficient method to predict the electronic excitation energies of BODIPY fluorescent dyes. *Journal of computational chemistry.* 2013; 34:566–575. [PubMed: 23115129]
31. Schmidt EY, et al. Synthesis and optical properties of 2-(benzo[b]thiophene-3-yl)pyrroles and a new BODIPY fluorophore (BODIPY = 4,4-difluoro-4-bora-3a,4a-diaza-s-indacene). *Chemistry.* 2009; 15:5823–5830. [PubMed: 19396897]
32. Zhu M, et al. Efficient tuning nonlinear optical properties: Synthesis and characterization of a series of novel poly(aryleneethynylene)s co-containing BODIPY. *Journal of Polymer Science Part A: Polymer Chemistry.* 2008; 46:7401–7410.
33. Bouit P-A, et al. Two-Photon Absorption-Related Properties of Functionalized BODIPY Dyes in the Infrared Range up to Telecommunication Wavelengths. *Advanced Materials.* 2009; 21:1151–1154.

34. Xu C, Zipfel W, Shear JB, Williams RM, Webb WW. Multiphoton fluorescence excitation: new spectral windows for biological nonlinear microscopy. *Proceedings of the National Academy of Sciences*. 1996; 93:10763–10768.
35. Porrès L, Mongin O, Blanchard-Desce M. Synthesis, fluorescence and two-photon absorption properties of multichromophoric boron-dipyrromethene fluorophores for two-photon-excited fluorescence applications. *Tetrahedron letters*. 2006; 47:1913–1917.
36. Zhang X, et al. Long-Wavelength, Photostable, Two-Photon Excitable BODIPY Fluorophores Readily Modifiable for Molecular Probes. *The Journal of organic chemistry*. 2013; 78:9153–9160. [PubMed: 23984818]
37. Loudet A, Burgess K. BODIPY dyes and their derivatives: syntheses and spectroscopic properties. *Chemical reviews*. 2007; 107:4891–4932. [PubMed: 17924696]
38. Sheik-Bahae M, Said AA, Wei T-H, Hagan DJ, Van Stryland EW. Sensitive measurement of optical nonlinearities using a single beam. *Quantum Electronics, IEEE Journal of*. 1990; 26:760–769.
39. Sutherland, RL. *Handbook of nonlinear optics*. CRC press; 2003.
40. Anand B, et al. Nonlinear optical properties of boron doped single-walled carbon nanotubes. *Nanoscale*. 2013; 5:7271–7276. [PubMed: 23817830]

- We examined absorption characteristics of BODIPY based  $\pi$ -conjugated pyrrole dyes.
- Pristine BODIPY possess saturable absorption behavior.
- 3,5-distyryl extended MeO<sub>2</sub>BODIPY dye depicts reverse saturable absorption.
- Observed nonlinear absorption coefficient is comparable to standard material ZnTPP.

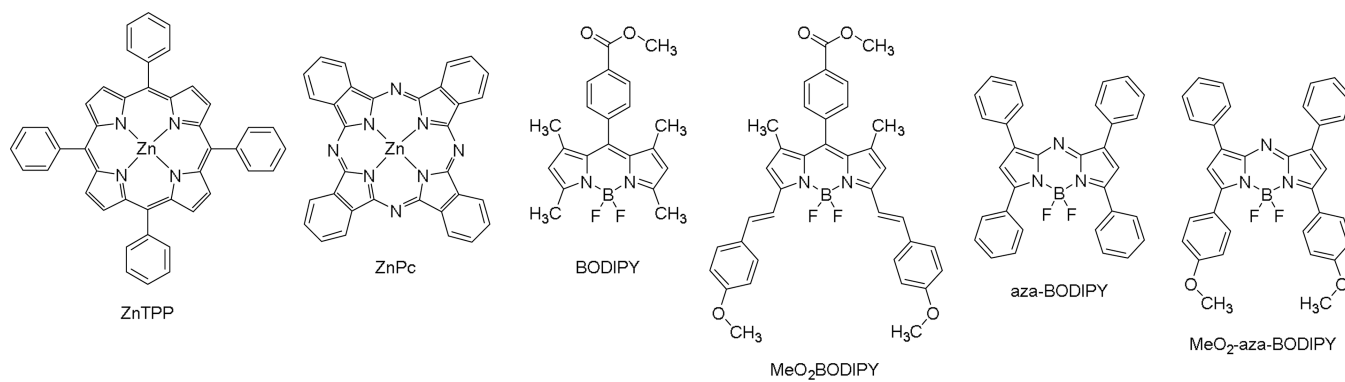


**Figure 1.**  
Structures of bis- and tetra-pyrrole dyes, and their aza analogues, investigated in this study.



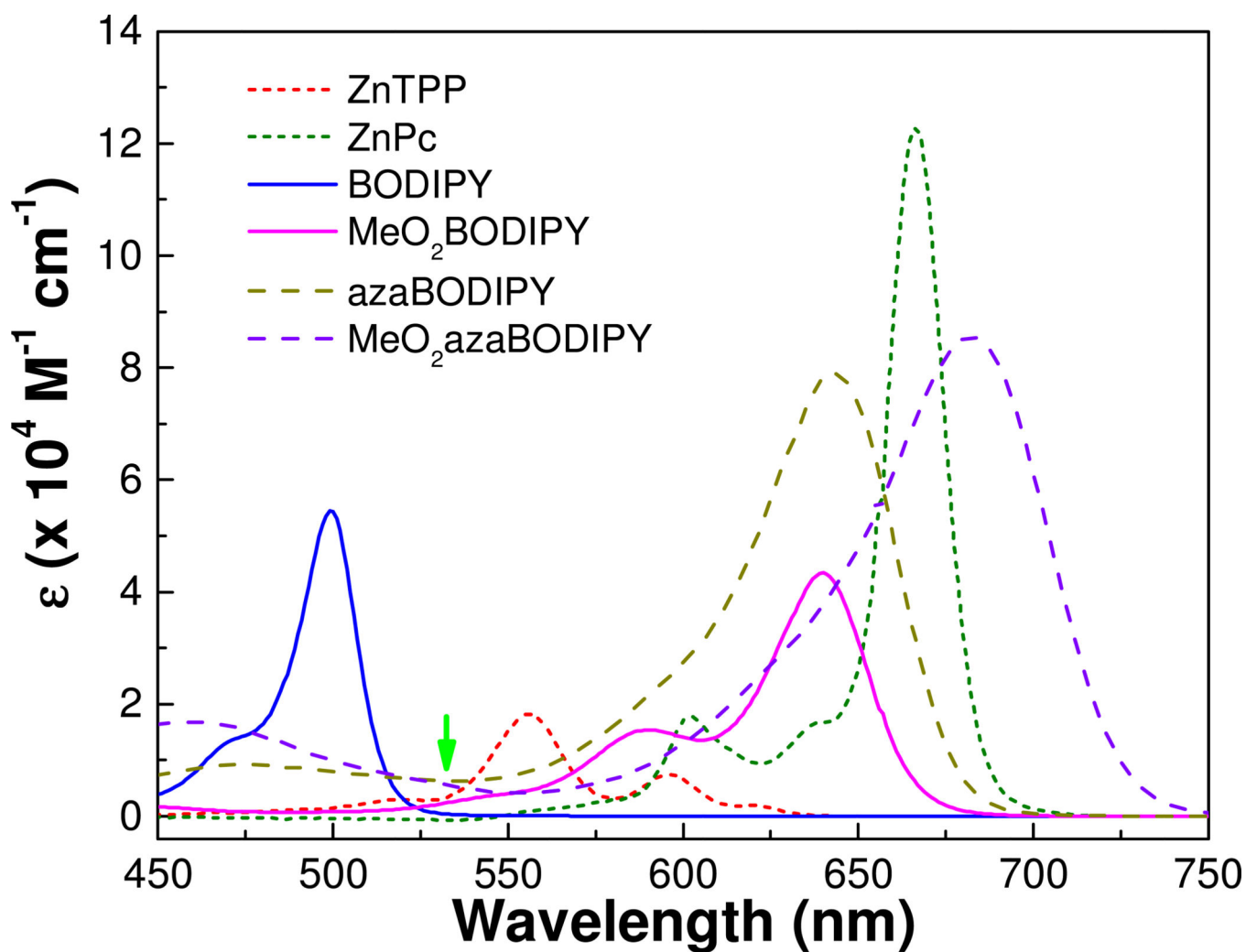


**Figure 2.** Electronic absorption spectra of the porphyrin, phthalocyanine, BODIPY and aza-BODIPY series recorded in tetrahydrofuran (arrow indicates laser excitation wavelength).

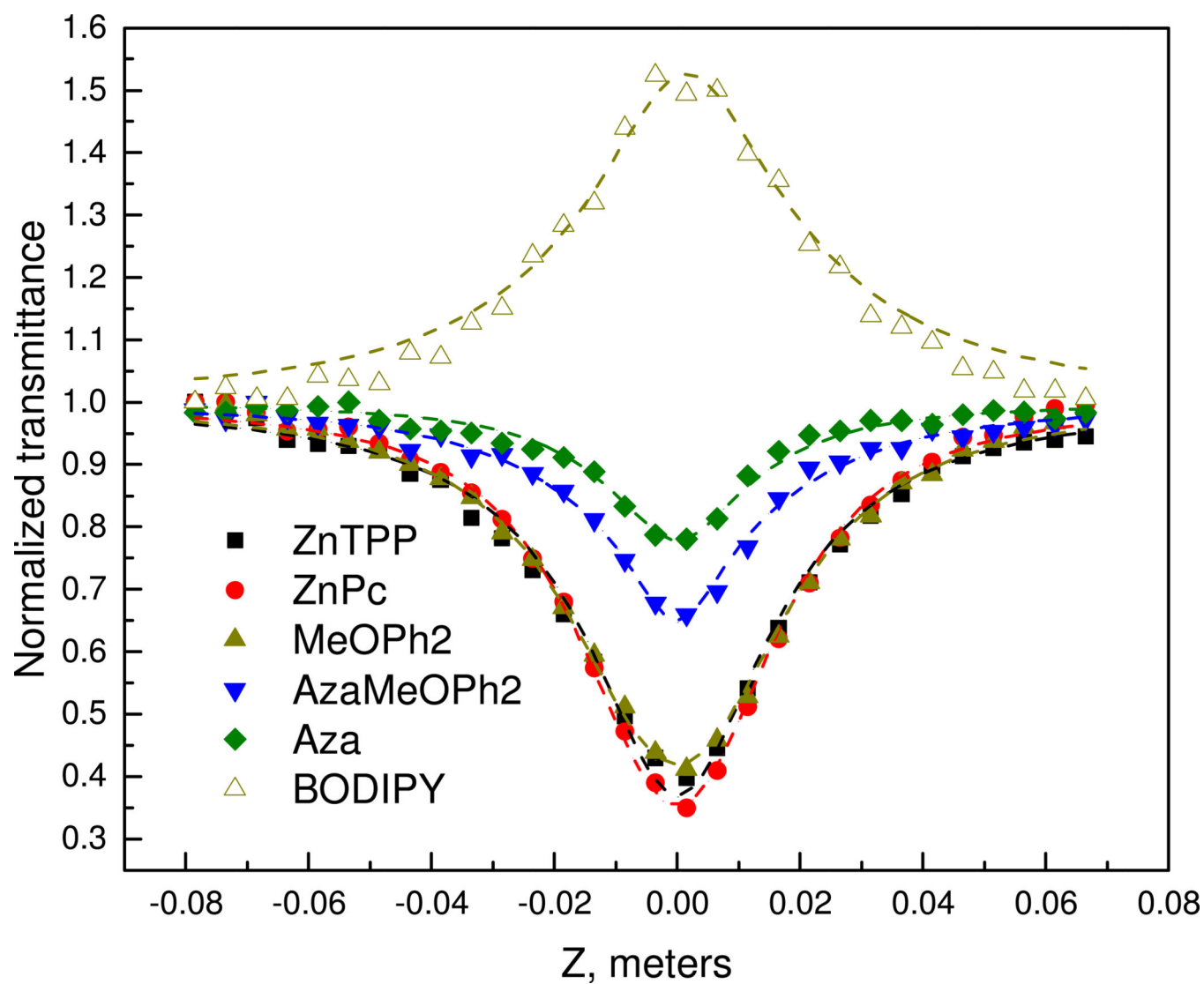


**Figure 3.** Open aperture Z-scan curves for the series of pyrrole dyes. The lines are theoretical fit to experimental data.

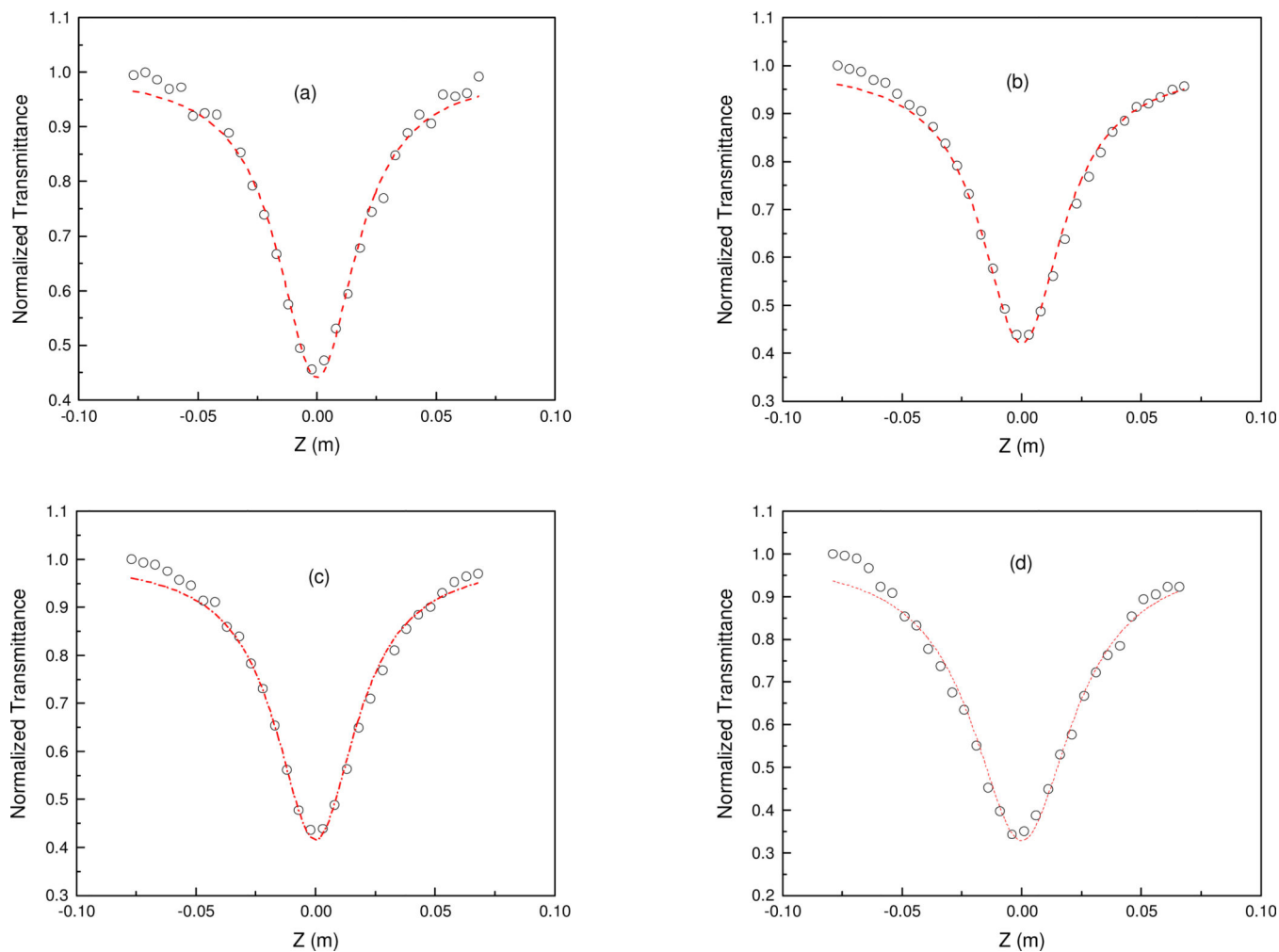


**Figure 4.**

Open aperture Z-scan curves for MeO<sub>2</sub>BODIPY at various on-axis intensities: (a)  $1.19 \times 10^{12} \text{ W/m}^2$ ; (b)  $2.1 \times 10^{12} \text{ W/m}^2$ ; (c)  $2.76 \times 10^{12} \text{ W/m}^2$ ; and (d)  $3.31 \times 10^{12} \text{ W/m}^2$ . The lines are theoretical fit to experimental data.

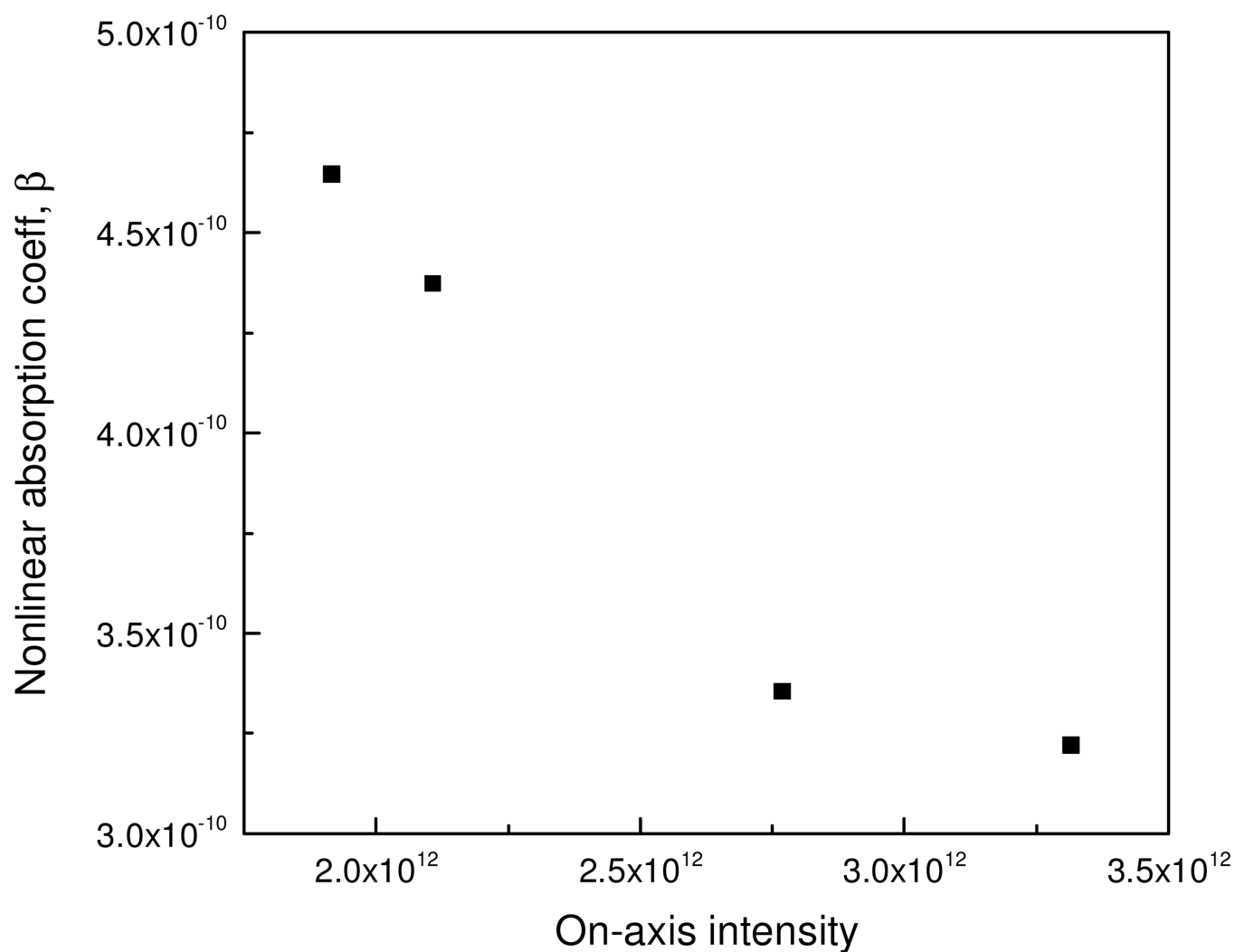


**Figure 5.** Variation of the nonlinear absorption coefficient  $\beta$  with on-axis peak intensity ( $I_0$ ). Decrease of  $\beta$  with  $I_0$  suggests ESA.

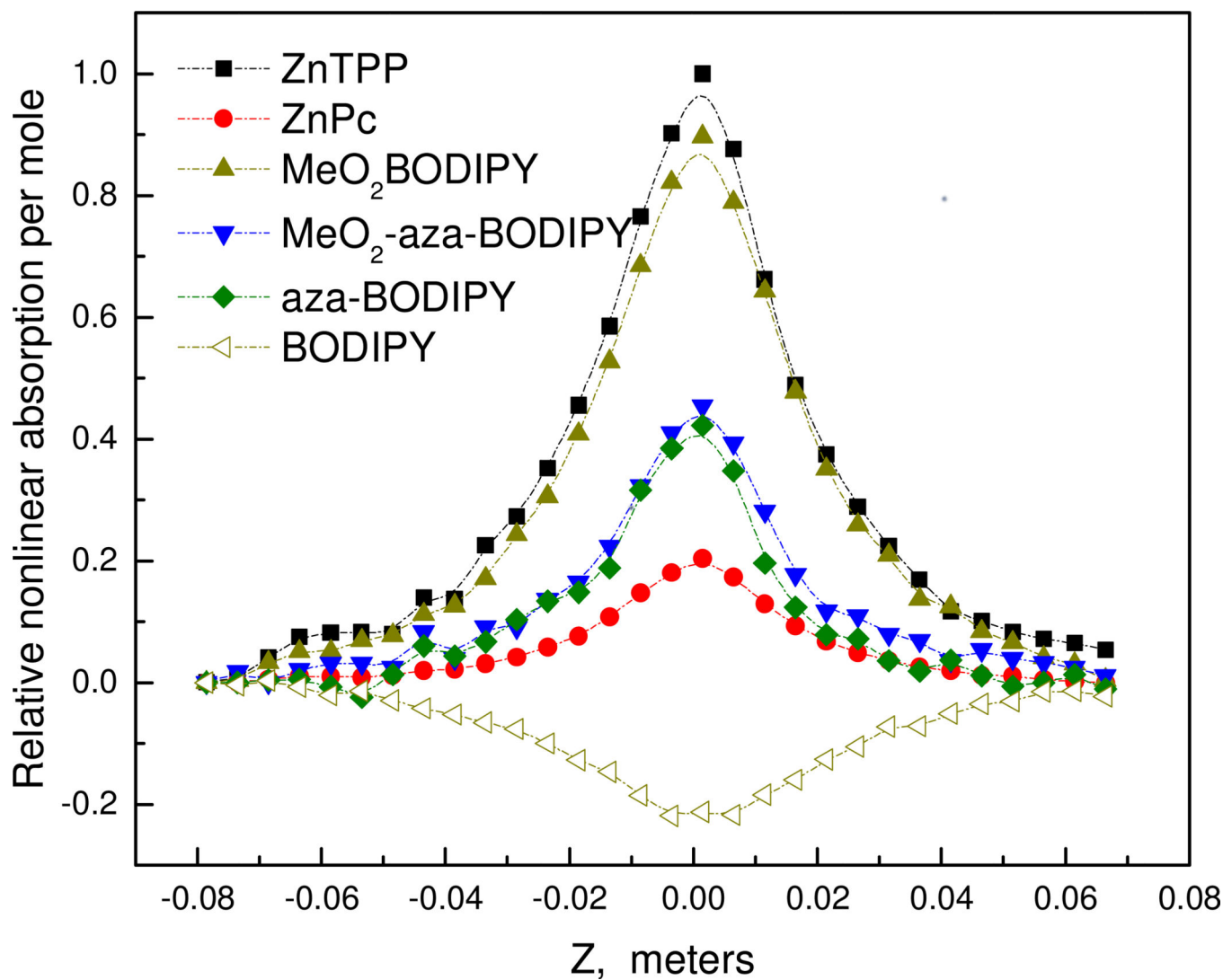


**Figure 6.**

Z-scan curves for the series of pyrrole dyes plotted as relative nonlinear absorption per mol with concentration of dyes taken into consideration. This plot effectively shows which dyes show the most efficient excited state absorption.

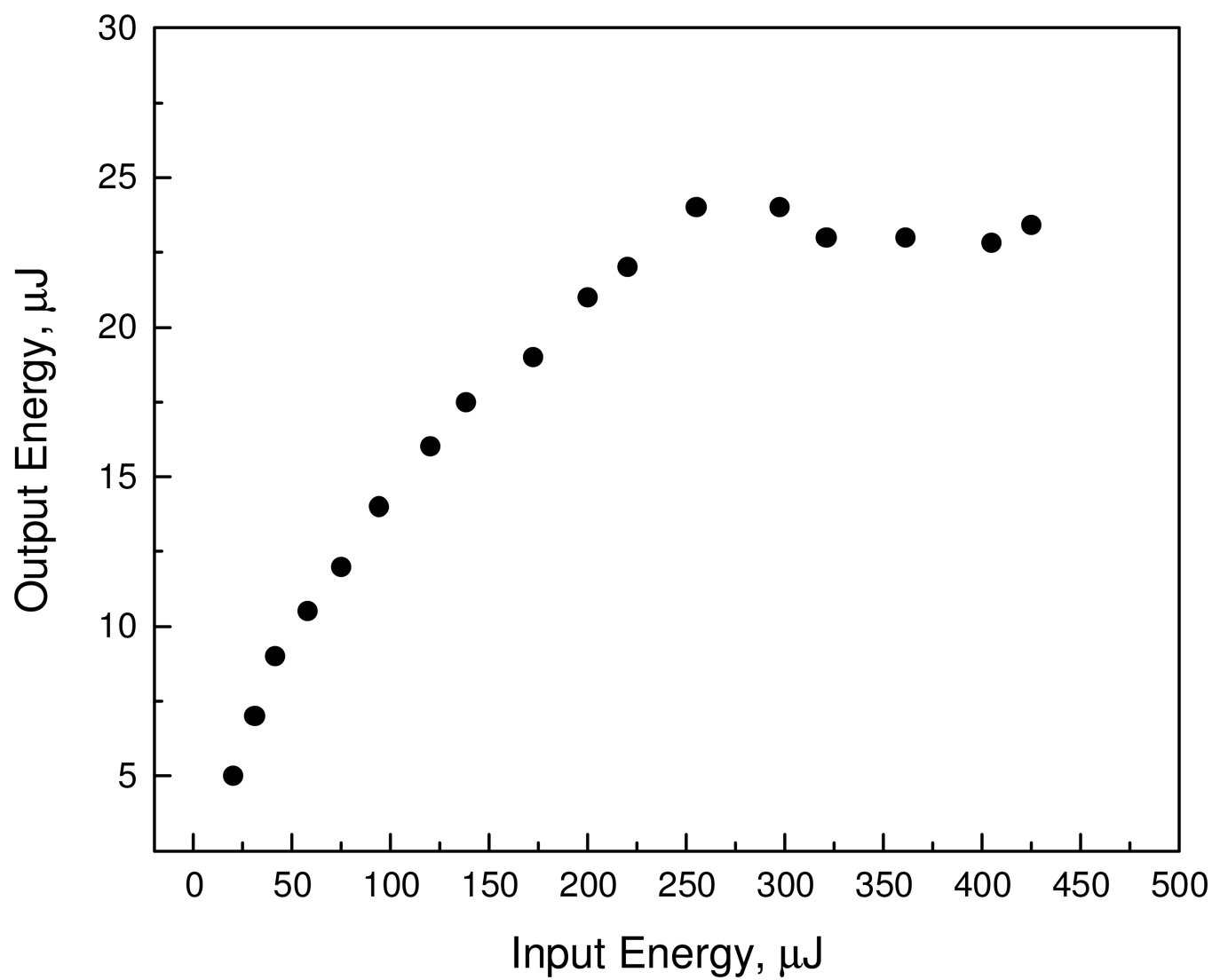


**Figure 7.**  
Optical power limiting behavior for MeO<sub>2</sub>BODIPY.

**Table 1**

Summary of nonlinear absorption coefficients for all dyes recorded using the Z-scan technique.

|                              | Concentration<br>(mol L <sup>-1</sup> ) | On axis intensity, I <sub>0</sub><br>W/m <sup>2</sup>         | ESA coefficient α <sub>2</sub><br>m/W |
|------------------------------|---|---|---------------------------------------|
| ZnPc                         | 1.71 × 10 <sup>-05</sup>                | 1.54 × 10 <sup>12</sup>                                       | 2.88 × 10 <sup>-10</sup>              |
| ZnTPP                        | 9.54 × 10 <sup>-05</sup>                | 1.93 × 10 <sup>12</sup>                                       | 4.97 × 10 <sup>-10</sup>              |
| MeO <sub>2</sub> BODIPY      | 1.83 × 10 <sup>-05</sup>                | 1.19 × 10 <sup>12</sup>                                       | 4.64 × 10 <sup>-10</sup>              |
|                              |   | 2.1 × 10 <sup>12</sup>  | 4.37 × 10 <sup>-10</sup>              |
|                              |   | 2.76 × 10 <sup>12</sup>                                       | 3.35 × 10 <sup>-10</sup>              |
|                              |   | 3.31 × 10 <sup>12</sup>                                       | 3.22 × 10 <sup>-10</sup>              |
| MeO <sub>2</sub> -aza-BODIPY | 1.65 × 10 <sup>-05</sup>                | 2.14 × 10 <sup>12</sup>                                       | 3.14 × 10 <sup>-10</sup>              |
| aza-BODIPY                   | 1.03 × 10 <sup>-05</sup>                | 2.78 × 10 <sup>12</sup>                                       | 1.71 × 10 <sup>-10</sup>              |
| BODIPY                       | 3.72 × 10 <sup>-05</sup>                | Saturation Intensity = 1.25×10 <sup>11</sup> W/m <sup>2</sup> |                                       |